Journal of mathematics and computer Science 7 (2013) 89 - 100

Contents list available at JMCS

Journal of Mathematics and Computer Science

Journal Homepage: www.tjmcs.com

Three-dimensional Numerical Analysis of Heat Transfer Characteristics of Solar Parabolic Collector With Two Segmental Rings

Seyed Ebrahim Ghasemi*, Ali Akbar Ranjbar, Abbas Ramiar

Department of Mechanical Engineering, Babol University of Technology, Babol, P.O. Box 484, Iran

Article history:
Received February 2013
Accepted March 2013
Available online April 2013

Abstract

In this article, the heat transfer characteristics of parabolic solar collector with two segmental rings has been investigated numerically. The effect of distance between porous two segmental rings on the heat transfer coefficient of the collector has been studied. The heat transfer fluid is Therminol 66 and the model is solved by RNG k–Ɛ turbulent model using Computational Fluid Dynamics (CFD) package, FLUENT. This numerical simulation is implemented for different distances between two segmental rings, the results show that use of two segmental rings in tubular solar absorber enhances the heat transfer characteristics of solar parabolic collector. Also by decreasing the distance between two segmental rings,the heat transfer coefficient increases.

Keywords: Solar Energy, Three-dimensional Numerical Analysis, Parabolic Trough Collector, Heat Transfer Characteristics, Two Segmental Rings.

1. Introduction

Solar energy has the greatest potential of all the sources of renewable energy especially when other sources in the country have depleted. Because of the desirable environmental and safety aspects it is widely believed that solar energy should be utilized instead of other alternative energy forms, even when the costs involved are slightly higher. Solar energy, radiant light and heat from the sun, has been harnessed by humans since ancient times using a range of ever-evolving technologies [1].

* Corresponding author:
E-mail: s.ebrahim.ghasemi@gmail.com

Currently, solar parabolic trough collector is employed for a variety of applications such as power generation [2], in dustrial steam generation [3], and hot water production [4].
Parabolic trough collector is preferred for steam generation because high temperatures can be obtained without any serious degradation of the collector's efficiency [5].
A solar parabolic trough concentrator focuses direct solar irradiation onto a tubular solar receiver positioned along the focal line, which absorbs and transfers the thermal energy to a heat transfer fluid (HTF) flowing inside the absorber tube. The temperature of the HTF can reach over 400℃ [6].
Faik A. Hamad studies experimentally the parabolic trough collector consists of a reflector and absorber [7]. The reflector 1m in length and 1m in width and the diameter of the absorber is 0.0125 m. The researcher found that the collector performance depends mainly on water mass flow rate, and there was no significant change when the mass flow rate becomes more than ten kilograms per hour. Edenburn predicted the efficiency of a parabolic trough collector by using an analytical heat transfer model for evacuated and nonevacuated cases [8]. The results showed good agreement with measured data obtained from SNL collector test facility [9].
Stuetzle proposed an unsteady state analysis of solar collector receiver to calculate the collector field outlet temperature [10]. The model was solved by discretizing the partial differential equations obtained by the energy balance. The results obtained showed that the overall match between the calculated and measured outlet temperature was good.
Vernon E. Dudley and Gregory J. Kolb in Sandia National Laboratory study theoretically and experimentally the parabolic trough solar collector to determine the collector efficiency and thermal losses with two types of receiver selective coatings combined with three different receiver configurations; glass envelope with either vacuum or air in the receiver annulus, and glass envelope removed from the receiver [11]. The researchers reach to decreased performance when the cermet selective coating, and progressively degraded as air was introduced into the vacuum annulus, and when the glass envelope was removed from receiver.
So in this paper, a numerical investigation of effect of distance between porous two segmental rings in the circular receiver with different boundary conditions for solar parabolic trough collector has been carried out. The heat transfer characteristics of tubular and porous two segmental rings receiver configurations have been evaluated to arrive to better heat transfer of the system.

2. Model Description

The schematic of solar parabolic system and the receiver of collector is shown in Figures 1 and 2 respectively.The solar radiation is concentrated onto the line circular absorber by a parabolic concentrator. The concentrated radiation is then transmitted to the heat transfer fluid by convection heat transfer in the receiver. The heat transfer characteristics of the parabolic trough collector can be improved by increasing the internal area and heat transfer rate. This can be achieved by incorporating porous two segmental rings inside the circular line receiver. The receiver is considered axisymmetric about its vertical axis.Therefore,only a half-section of the absorber is considered for numerical modeling.

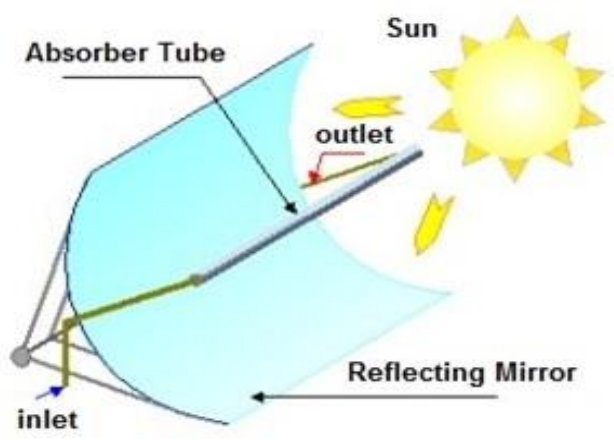

Figure1. solar parabolic system

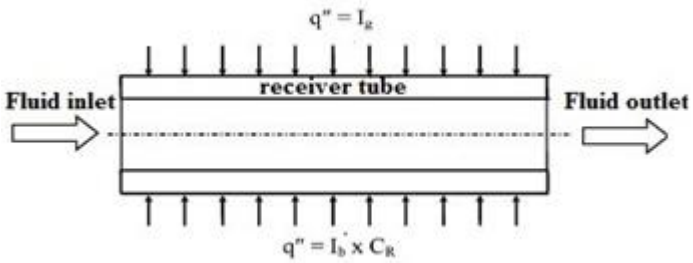

Figure 2. receiver of solar parabolic collector

For the numerical simulation, the flow is considered as hydrodynamically developed and thermally developing flow. The properties of the heat transfer fluid and absorber material are assumed constant. The thermo-physical properties and geometrical parameters of the absorber are illustrated in Tables 1 and 2 respectively.

Table 1. Thermophysical properties of heat transfer fluid, two segmental rings and absorber

	Heat Transfer fluid (Therminol 66)	Two segmental rings and absorber (Stainless steel)
Density (kg/m^3)	899.5	8027
Specific heat (J/kg.k)	2122	500
Viscosity $(N.s/m^2)$	0.00106	-
Thermal conductivity $(W/m.k)$	0.107	20

Table 2. Geometrical parameters of the porous three segmental rings and absorber

Length of the receiver (m)	2
Inside diameter of the receiver (mm)	68
Thickness of the porous three segmental rings (mm)	3
Outside diameter of the receiver (m)	74
Glass cover diameter (mm)	120

2.1. Governing Equations

The governing equations for steady, turbulent, incompressible, forced convection in receiver are given as [12] Continuity equation for porous medium:

$$\nabla u = 0 \tag{1}$$

Momentum equation for forced convection in the porous medium:

$$\frac{\rho_f}{\varphi}\nabla\left(\frac{u.u}{\varphi}\right) = -\nabla P + \frac{\mu}{\varphi\rho_f}\nabla^2 u - \frac{\mu}{K_P}u - \frac{\mu}{K_P^{1/2}}\rho_t u^2 \tag{2}$$

Energy equation for solid phase:

$$(1-\varphi)\nabla(k_s \nabla T_s) = 0 \tag{3}$$

for fluid phase:

$$(\rho C_p)_f u\nabla T_f = \varphi\nabla(k_f \nabla T_f) \tag{4}$$

In renormalization-group (RNG) k– Ɛ model, the momentum equation involving turbulent stresses can be solved by using Reynolds Averaged Navier Stokes (RANS) equations. The RANS equations are time-averaged equations of motion for turbulent fluid flow. These equations can be used with approximations based on the properties of flow turbulence to give approximate averaged solutions to the Navier–Stokes equations. For an incompressible flow of Newtonian fluid, these equations can be written as [13]:

$$\frac{\partial}{\partial x_j}\left(\overline{u_i u_j}\right) = \frac{-1}{\rho_f}\frac{\partial \bar{P}}{\partial x_i} + \frac{\partial}{\partial x_j}\left[\mu_{eff}\left(\frac{\partial u_i}{\partial x_j} + \frac{\partial u_j}{\partial x_i}\right)\right] \tag{5}$$

Where $\mu_{eff} = \mu + \mu_t, \mu_t = C_\mu \frac{K^2}{\varepsilon}, C_\mu = 0.0845, K = 0.71\varepsilon^{2/3}L^{2/3}$

The values of k and ε which are determined by transport equations

$$\overline{u_i}\frac{\partial k}{\partial x_i} = \upsilon_t S^2 - \varepsilon + \frac{\partial}{\partial x_i}\left(\alpha_t \upsilon_t \frac{\partial k}{\partial x_i}\right) \tag{6}$$

And

$$\overline{u_i}\frac{\partial \varepsilon}{\partial x_i} = \frac{C_{\varepsilon 1}\varepsilon\upsilon_t}{k}S^2 - \frac{C_{\varepsilon 2}\varepsilon^2}{k} - R + \frac{\partial}{\partial x_i}\left(\alpha_t \upsilon_t \frac{\partial \varepsilon}{\partial x_i}\right) \tag{7}$$

The parameter α_t is inverse Prandtl number for turbulent transport. The turbulent viscosity ν_t is given by:

$$\nu_t = (\nu_{eddy} - \nu_o) \tag{8}$$

R is given by

$$R = \frac{C_\mu \eta^3 (1 - \eta/\eta_o)}{1 + \psi\eta^3} \frac{\varepsilon^2}{k} \tag{9}$$

The RNG theory gives the values of constants as

$$\eta = Sk/\varepsilon, \eta_0 = 4.38, S^2 = 2S_{ij}S_{ij}, C_{\varepsilon 1} = 1.42, C_{\varepsilon 2} = 1.68, \alpha_t = 1.39, \psi = 0.012$$

By inserting porous medium increases the heat transfer coefficient of the receiver.

2.2. Boundary Conditions

The receiver is considered symmetric about its vertical axis. Therefore only half section of receiver has been considered for numerical modeling.
The following boundary conditions are applied in the receiver model:
(i) Inlet boundary condition:
The flow is having uniform velocity at atmosphere temperature at the receiver inlet:

$$u = U_{in}, T_f = T_{in} = 330k @ L = 0$$
$$0 \le r \le \frac{d}{2} \quad , \quad -90° < \theta \le 90° \tag{10}$$

(ii) Wall boundary condition:
No-slip conditions exist at inside the pipe wall

$$u = 0 @ r = \frac{d}{2}$$
$$90° \le \theta \le -90° \quad , \quad 0 \le L \le 2 \tag{11}$$

A uniform heat-flux is applied at the pipe outer surface
(a) The top half periphery of the receiver is subjected to

$$q'' = I_g$$
$$0 \le \theta \le 90° \quad , \quad 0 \le L \le 2 \tag{12}$$

(b) The bottom half periphery of the receiver is subjected to

$$q'' = I_b C_R$$
$$-90° \le \theta \le 0° \quad , \quad 0 \le L \le 2 \tag{13}$$

Where $I_b = 650\, W/m^2$, $I_g = 750\, W/m^2$ and $C_R = \frac{A_p}{A_r}$

(iii) Zero pressure gradient condition is employed across the outlet boundary.
(iv) Symmetry boundary conditions are applied for the receiver

3. Numerical Implementation

The governing equations were solved using finite volume method by segregated implicit solver with first order formulation with CFD commercial software FLUENT-6.2 [15]. The segregated solver solves conservation governing equations independently, and it is applicable for the incompressible flow. The geometrical model is created and meshed using commercial software GAMBIT with a quadrilateral cell (Fig. 3. (a)). The triangular mesh is used for the inlet and outlet faces, whereas the hybrid/tetragonal mesh are used for volume mesh (Fig. 3.(b)). A 3-D steady state turbulent RNG k–Ɛ model with standard wall functions was used for the simulation of forced convection in the receiver.
The RNG turbulence model is more responsive to the effects of rapid strain and streamlines curvature, flow separation, reattachment and recirculation than the standard k– Ɛ model. The RNG k– Ɛ model gives the best predictions of all the two-equation models as far as the velocity field, the turbulence kinetic energy and the recirculation length are concerned [16]. The RNG derived k– Ɛ model gave very good predictions for a pipe with sudden expansion, especially when non-equilibrium wall-functions were implemented [17]. Therefore RNG k– Ɛ turbulent model is adapted for the parabolic trough receiver system. The discretization scheme used for pressure is body force weighted to take the density variations in consideration. The solution is based on pressure correction method and uses SIMPLEC algorithm [16]. The first order upwind differencing scheme is used for momentum and energy equations. The solution is considered to be converged sufficiently when the normalized residual of 10^{-3} for momentum and mass and 10^{-6} for energy equations.
The simulations were carried out for fully developed flow conditions Heat transfer coefficient from the receiver to the fluid is given by:

$$h_f = \frac{q''}{T_{wi} - T_{ref}} \tag{14}$$

The Nusselt number is given by:

$$Nu = \frac{h_f d}{k_f} \tag{15}$$

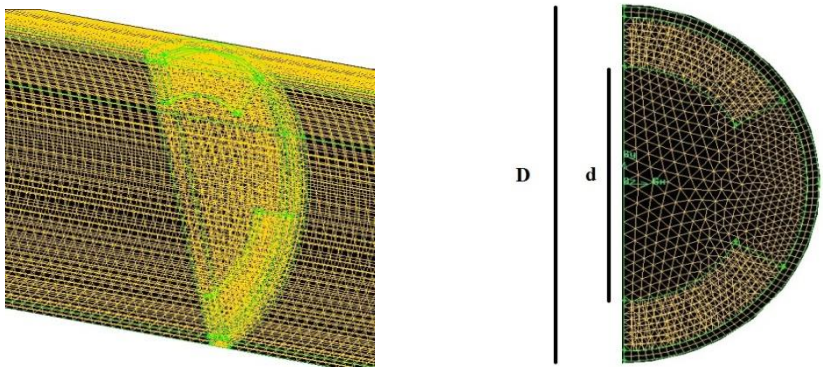

(a) around the two segmental rings **(b)inlet and outlet faces**

Figure 3. Grid generation for porous two segmental rings receiver

3.1. Grid Independency

The grid independent study was carried out before the actual simulation of the 3-D tubular receiver. After the study, it is found that 1,328,609 cells are sufficient with minimum deviation with the previous values for the tubular receiver. Similarly, it is found that 1,753,150 cells are sufficient for the porous two segmental rings receiver.

3.2. Code Validation

The Nusselt number obtained from the present numerical code has been validated by using the Nusselt number estimated from the Gnielinski equation and applying uniform heat flux over the entire surface of the tubular receiver. The Gnielinski equation for heat transfer fluid is given by [18]:

$$Nu = \frac{\left(\frac{f}{8}\right)(\mathrm{Re}-1000)\,\mathrm{Pr}}{1+12.7\left(\frac{f}{8}\right)^{1/2}\left(\mathrm{Pr}^{2/3}-1\right)} \quad \text{for} \quad 3000 \le \mathrm{Re} \le 5\times10^{6} \quad \text{and} \quad 0.5 \le \mathrm{Pr} \le 2000 \tag{16}$$

Where we have:

$$f = \left(0.79Ln\,\mathrm{Re}-1.64\right)^{-2} \tag{17}$$

$$\mathrm{Re} = \frac{\rho_f u D}{\mu} \tag{18}$$

The Nusselt number comparison of the tubular receiver (uniform heat flux over the receiver periphery) with the Gnielinski correlation is shown in Figure 4. The model is in reasonable agreement with the Gnielinski equation and deviates only 8 % for all the Reynolds numbers.

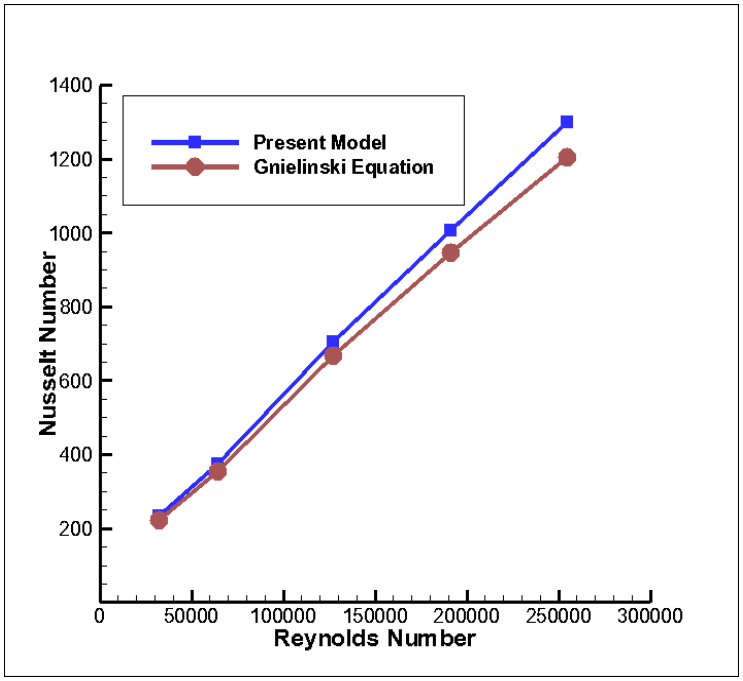

Figure 4. Validation of present model with Gnielinski equation.

The numerical code is also validated with the Akansu [19] model is shown in Fig. 5. Akansu studied heat transfer and pressure drop for porous ring turbulators in a circular pipe for different geometric parameters. In present numerical model,the convective heat transfer coefficient deviates maximum of 9.3 % with Akansu for all the Reynolds numbers.

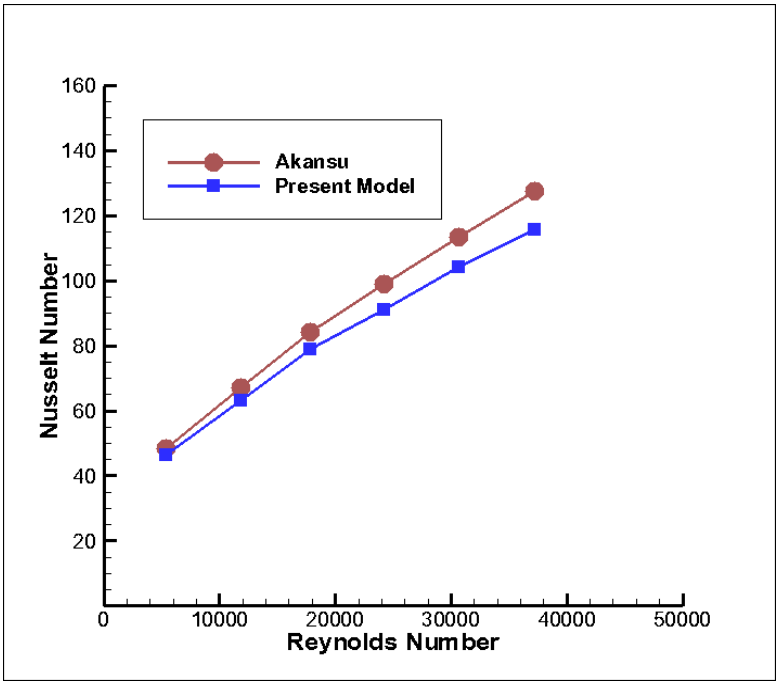

Figure 5. Validation of present model with Akansu model.

4. Results and Discussion

The numerical simulation was carried out for a receiver configuration with porous two segmental rings. These two segmental rings produce turbulence in the receiver, which increases heat transfer area and effective thermal conductivity. These effects are responsible for a higher heat transfer coefficient in porous receivers than in ordinary tubular receivers. The effect of distance between porous two segmental rings (Q) on the Nusselt number in absorber is shown in Figs. 6, 7, 8 and 9.

Figs. 6, 7, 8 and 9 illustrates the Nusselt number versus the Reynolds number for four different distances between porous two segmental rings (Q=0.75d, Q=d, Q=1.5d and Q=2d).

In each figures the inside diameter of the porous two segmental rings is constant, i.e.

D/D=0.6, d/D=0.7, d/D=0.8 and d/D=0.9

Where d is inner diameter of two segmental rings and D is absorber inner diameter.

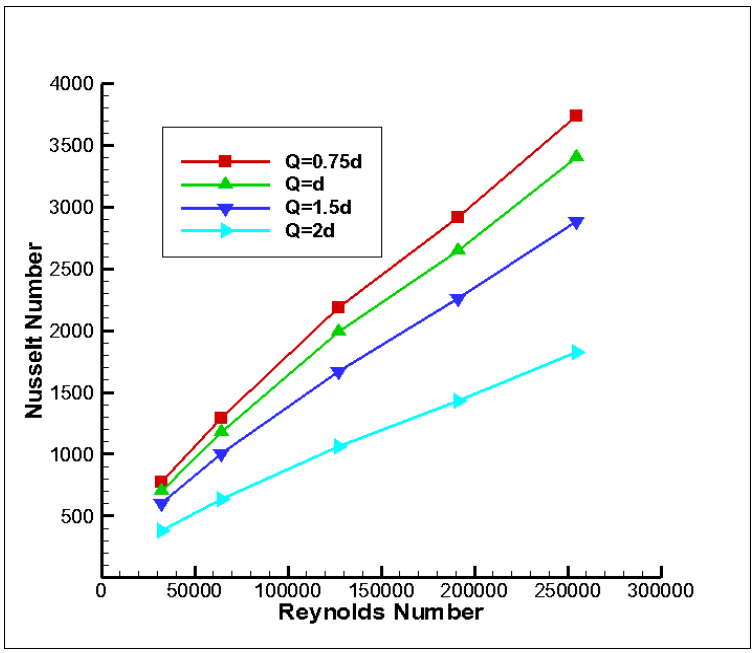

Figure 6. Effect of distance between two segmental rings on Nusselt number for d/D=0.6

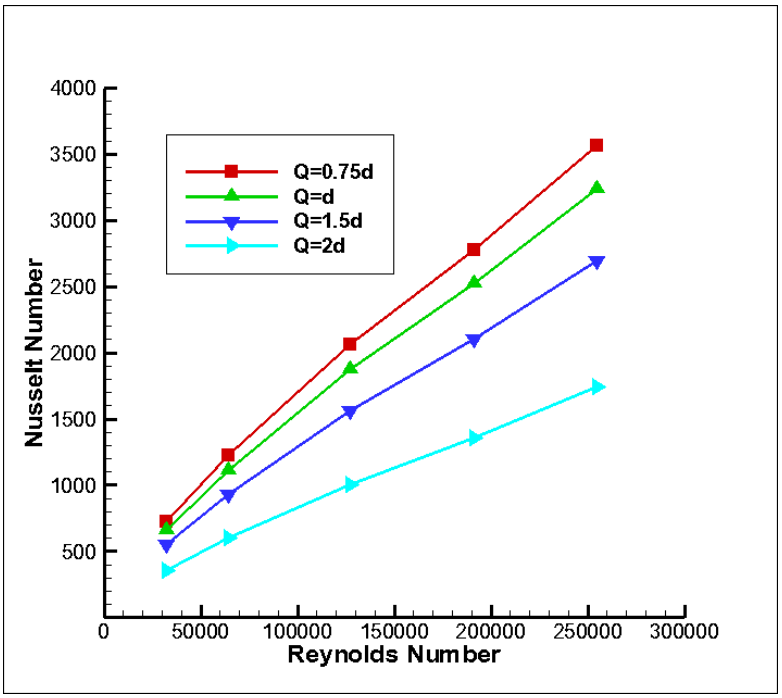

Figure 7. Effect of distance between two segmental rings on Nusselt number for d/D=0.7

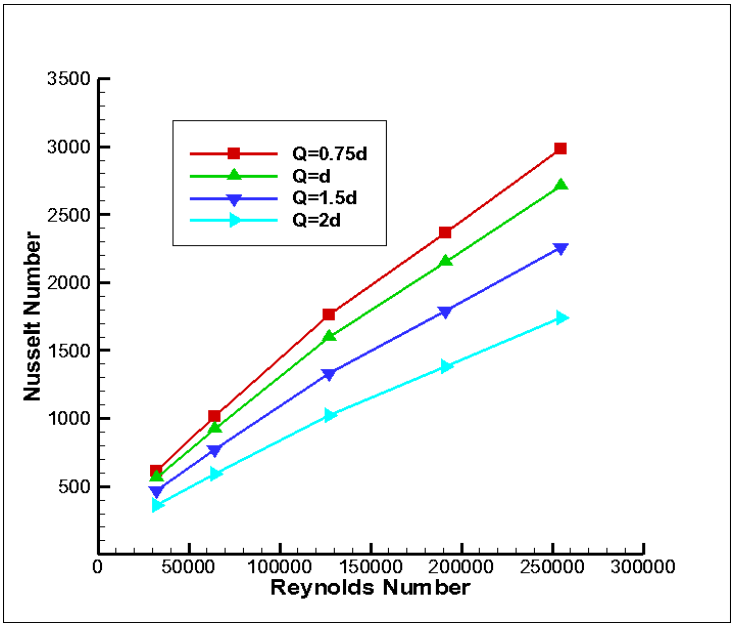

Figure 8. Effect of distance between two segmental rings on Nusselt number for d/D=0.8

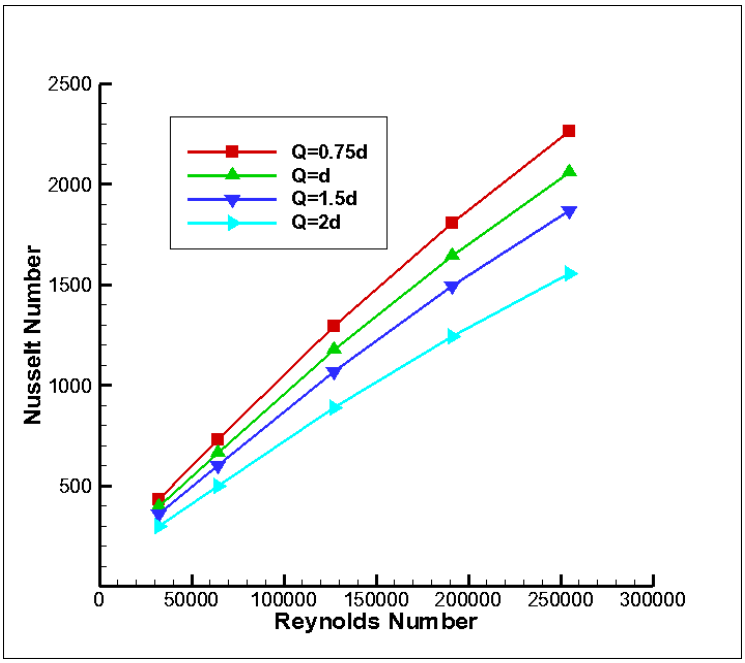

Figure 9. Effect of distance between two segmental rings on Nusselt number for d/D=0.9

It is apparent from Figs.6, 7, 8 and 9 that the Nusselt number enhances by decreasing of distance between two segmental rings. As the distance between two consecutive porous two segmental rings decreases the number of porous two segmental rings in the receiver increases, hence heat transfer area increases.

Also the results show that by increasing the inner diameter of two segmental rings the Nusselt number decreases. Heat transfer increases with increases of Reynolds number.

The temperature contours at the receiver outlet for different inner diameter of two segmental rings and (Q=2d for Reynolds number 32458) are shown in Figure 10.

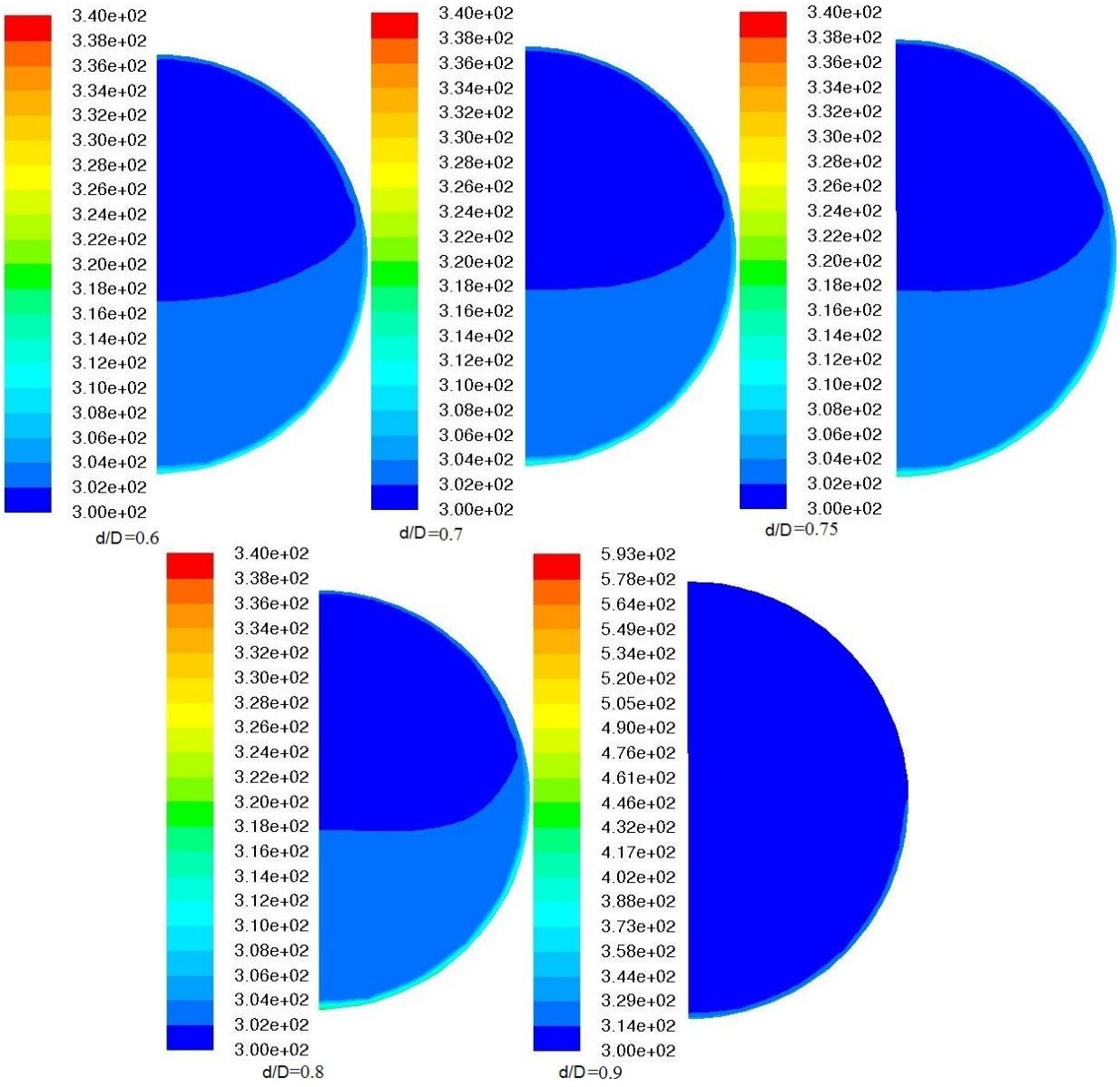

Figure 10. Temperature contours at the outlet of the two segmental rings

5. Conclusion

Numerical analysis of the heat transfer for porous two segmental rings placed in the absorber tube of the solar parabolic collector is provided for Reynolds numbers ranging from 32458 to 254317. The heat transfer fluid is Therminol 66 and four different inner diameter of segmental rings and four different distances between porous two segmental rings are considered. The thermal efficiency of the solar parabolic system has been improved by insertion of porous two segmental rings and the results show that the Nusselt number reduces with increases of the distance between two segmental rings.

Consequently, the maximum Nusselt numbers depend on the Reynolds number, inner diameter and distance between porous two segmental rings. The higher heat transfer enhancement was obtained in the case of Q and d/D being 0.75d and 0.6 respectively.

Refrences:

[1] R.Nasrin, M.A. Alim, "DUFOUR-SORET EFFECTS ON NATURAL CONVECTION INSIDE A SOLAR COLLECTOR UTILIZING WATER-CUO NANOFLUID", International Journal of Energy & Technology 4 (23) 1–10, **(2012).**

[2] F.Lippke, "Direct Steam Generation in Parabolic Trough Solar Power Plants: Numerical Investigation of the Transients and the Control of a Once-Through System", Journal of Solar Energy Engineering, 118, pp. 9-14, **(1996)**.

[3] E.K.May, L. M.Murphy, "Performance Benefits of the Direct Generation of Steam in Line-Focus Solar Collectors, Journal of Solar Energy Engineering, 105: pp. 126-133, **(1983)**.

[4] S.Kalogirou, S.Lloyd, "Use of Solar Parabolic trough Collectors for Hot Water Production in Cyprus. A feasibility study, Renewable Energy, 2, pp. 117-124, **(1992)**.

[5] S.Kalogirou, S.Lloyd, J.Ward, P.Eleftheriou, "Design and Performance Characteristics of a Parabolic Trough Solar Collector System", Applied Energy, 47, pp. 341-354, **(1994)**.

[6] H.Price, E.Lupfert, D.Kearney, E. Zarza,G. Cohen,R. Gee, and R.Mahoney , "Advances in Parabolic Trough Solar Power Technology," J. Sol. Energy Eng., 124(2), pp. 109–125,**(2002)**.

[7] F. A. Hamad, "The Performance Of Cylindrical Parabolic Solar Concentrator", Solar Energy Res. Vol. 5, No. 2, P.P. (1-19), Basrah, Iraq, **(1987)**.

[8] MW.Edenburn, "Performance analysis of a cylindrical parabolic focusing collector and comparison with experimental results", Solar Energy, 18(5):437–44, **(1976)**.

[9] R.Pope, W.Schimmel, "An analysis of linear focused collectors for solar power", In: Eighth intersociety energy conversion engineering conference. Philadelphia, PA,p. 353–9,**(1973)**.

[10] T.Stuetzle, "Automatic Control of the 30 MWe SEGS VI Parabolic Trough Plant",Master thesis, University of Wisconsin-Madison, College of Engineering,**(2002)**.

[11] V.E. Dudley, G.J. Kolb, A.R. Mahoney, T.R. Mancini, C.W. Matthews, M. Sloan, D. Kearney, Test results: SEGS LS-2 solar collector, Report of Sandia National Laboratories (SANDIA-94-1884), **(1994)**.

[12] DA.Nield, A.Bejan, "Convection in porous media", New York: Spinger–Verlag, **(1998).**

[13] G.Biswas, V.Eswaran, "Turbulent flows fundamentals experiments and modeling", New Delhi: Narosa publishing house, **(2002)**.

[14] Fluent Inc., Fluent 6.2 user's guide. Lebanon: NH, **(2005).**

[15] B.Zheng, CX.Lin, MA.Ebadian, "Combined turbulent forced convection and thermal radiation in a curved pipe with uniform wall temperature", Numer Heat Transfer A – Appl; 44:149–67, **(2003).**

[16] ED.Koronaki, HH.Liakos, MA.Founti, NC.Markatos, "Numerical study of turbulent diesel flow in a pipe with sudden expansion", Appl Math Model; 25:319–33, **(2001).**

[17] V.Gnielinski, "New equations for heat and mass transfer in turbulent pipe flow and channel flow", Int Chem Eng 16: 359–368, **(1976).**

[18] S.A.Akansu, "Heat Transfers and Pressure Drops for Porous-Ring Turbulators in a Circular Pipe", Applied Energy, vol. 83, pp. 280–298, **(2006)**.